Numerical Study on the Motion of Azimuthal Vortices in Axisymmetric Rotating Flows

Yong Kweon Suh*

Division of Mechanical and Industrial System Engineering, Dong-A University, 840 Hadan-dong, Saha-gu, Busan 604-714, Korea

A rich phenomenon in the dynamics of azimuthal vortices in a circular cylinder caused by the inertial oscillation is investigated numerically at high Reynolds numbers and moderate Rossby numbers. In the actual spin-up flow where both the Ekman circulation and the bottom friction effects are included, the first appearance of a seed vortex is generated by the Ekman boundary-layer on the bottom wall and the subsequent roll-up near the corner bounded by the side wall. The existence of the small vortex then rapidly propagates toward the inviscid region and induces a complicated pattern in the distribution of azimuthal vorticity, i.e. inertial oscillation. The inertial oscillation however does not deteriorate the classical Ekman-pumping model in the time scale larger than that of the oscillatory motion. Motions of single vortex and a pair of vortices are further investigated under a slip boundary-condition on the solid walls. For the case of single vortex, repeated change of the vorticity sign is observed together with typical propagation of inertial waves. For the case of a pair of vortices with a two-step profile in the initial azimuthal velocity, the vortices' movement toward the outer region is resisted by the crescent-shape vortices surrounding the pair. After touching the border between the core and outer regions, the pair vortices weaken very fast.

Key Words : Rotating Flows, Inertial Oscillation, Spin-up, Circular Cylinder, Azimuthal Vortex

1. Introduction

Rotating flows are ubiquitous in natural and technological environment. In view of its consequence in engineering and scholarly interest, it has drawn much attentions of the fluid dynamicists from long time ago. Its application can be found in broad areas such as turbomachinery, oceanic flows, atmospheric flows, the motion of liquid fuel within space crafts, mantle movement inside the Earth, and spin coating, etc. In more specific terms, the rotating flows are characterized by relative flows under a background rotation; the ratio of the representative magnitude of relative-flow velocity and that of the background rotational velocity is defined as the Rossby number. The relative flows are intrigued by various mechanisms. In the spin-up flows, the rotational speed is just increased abruptly, and the subsequent flow development, i.e. decay, in time becomes the primary interest. The relative flows can be generated by other forces such as the buoyant force, the magnetic force, and the surface force driven by winds. Among these, the body force given by the increase (or decrease in the 'spin-down' case) of the rotational speed presents the most fundamental subject known as 'spin-up' flow.

Early investigation on the spin-up flows has focussed on axisymmetric containers and aimed to understand the basic underlying mechanism

* **E-mail** : yksuh@daunet.donga.ac.kr
TEL : +82-51-200-7648; **FAX** : +82-51-200-7656
Division of Mechanical and Industrial System Engineering, Dong-A University, 840 Hadan-dong, Saha-gu, Busan 604-714, Korea. (Manuscript **Received** July 9, 2003; **Revised** November 17, 2003)

associated with the decaying of the primary flow. Greenspan and Howard (1963) studied on the spin-up of fluid in between two infinite parallel plates. They showed that at small Rossby numbers the linearized version of the governing equations can well predict the spin-up time. Wedemeyer (1964) proposed an approximation method for treating the non-linear equations for the spin-up from rest (Rossby number =1). He applied his approximation method to the circular-cylinder case and showed that during the spin-up process a shear discontinuity front appears near the side wall between the regions of positive and negative vorticity and it moves toward the central axis.

On the other hand, recently there have been increased interests in improving the Ekman pumping models (e.g. Hart 1995, 2000; Zavala Sanson and van Heijst 2000; Suh and Choi 2002). The proposed models compare well with experimental results even in the non-axisymmetric container such as a rectangle. However it still demands further improvement especially in the very beginning stage and at moderate Rossby numbers. As a fundamental motivation of this study, it is assumed that the inertial oscillations (see e.g. Greenspan 1968) may be one of the key reasons for the discrepancy. For instance Cederlöf (1988) suggested that the inertial oscillation in the spin-up inside a circular cylinder may give rise to Lagrangian drift motion. Dolchanskii, Krymov and Manin (1992) showed experimentally that considerable amount of inertial oscillations takes place in the circular cylinder of small ratio of height to a diameter. The inertial oscillations also have been observed numerically by Hyun, Fowlis and Warn-Varnas (1982). However there have been no detailed reports on the study of inertial oscillations and its effect on the decay of the primary azimuthal flows.

In the literature however most studies concerning the inertial oscillation are oriented to the structure of the wave field, and no studies have been given to its connection with the bizarre behavior of the horizontal vortices (here the term 'horizontal' indicates 'normal' to the rotational axis which is vertical) within the rotating fluids.

The present study is thus purposed to investigate the motion of the horizontal vortices and the influence of the inertial oscillation to the vortices' motions. For simplicity, we focuss our attention to the axisymmetric-flow configuration, and use numerical methods to obtain the solutions of the basically two-dimensional Navier-Stokes equations. In Section 2, the problem is formulated and the numerical methods are described. To verify the two-dimensional numerical code, we also employed one-dimensional equations by using the Ekman pumping models developed by Suh and Choi (2002). The Wedemeyer's solution is also presented in this section for further verification of the two-dimensional code. A simple linear analysis for the inertial oscillation is given in Section 3. The numerical results and discussions are then presented in Section 4, and final conclusions are summarized in Section 5.

2. Formulation, Numerical Methods and Analysis

2.1 Two-dimensional equations

Consider a circular cylinder of radius R containing a viscous fluid of density ρ and viscosity ν with a free surface and rotating in a constant angular velocity Ω_s. The flow is maintained in a solid body rotation. Then at an instant of time the rotational speed is suddenly increased to $\Omega_0=\Omega_s+\Delta\Omega$. Assuming that the flow is axisymmetric and taking $1/\Delta\Omega$, R, $R\Delta\Omega$, $\rho R^2\Omega\Delta\Omega$ as the reference quantities for the time, length, velocity, and pressure, we can write the non-dimensional governing equations as follows.

$$\frac{\partial v}{dt}+u\frac{\partial v}{\partial r}+w\frac{\partial v}{\partial z}+\frac{uv}{r}+\frac{2}{\varepsilon}u=\frac{1}{Re}\triangle_2 v \quad (1)$$

$$\frac{\partial \zeta}{\partial t}+u\frac{\partial \zeta}{\partial r}+w\frac{\partial \zeta}{\partial z}-\frac{u\zeta}{r}+\frac{1}{r}\frac{\partial v^2}{\partial z}+\frac{2}{\varepsilon}\frac{\partial v}{\partial z}=\frac{1}{Re}\triangle_2\zeta \quad (2)$$

$$\triangle_2\psi=-\zeta \quad (3)$$

where t is time, (r, z) the coordinates along the radial and axial directions, respectively, u, v and w the velocity components in the radial,

azimuthal, and axial directions, respectively, p the pressure, and ζ the azimuthal vorticity; $\zeta=\partial w/\partial r-\partial u/\partial z$. Here the coordinates are corotating with the circular cylinder. The stream function ψ is related to the velocity components as

$$u=\frac{\partial\psi}{\partial z},\ w=-\frac{1}{r}\frac{\partial r\psi}{\partial r} \tag{4}$$

and the operator $\triangle_2$ denotes $\triangle_2=\partial^2/\partial r^2+\partial/r\partial r-1/r^2+\partial^2/\partial z^2$. Three dimensionless parameters are Re, the Reynolds number, ε, the Rossby number and h, the dimensionless liquid depth, defined as

$$Re=\frac{R^2\Delta\Omega}{\nu},\ \varepsilon=\frac{\Delta\Omega}{\Omega_0},\ h=\frac{H}{R} \tag{5}$$

Impermeable conditions are employed on all the boundaries surrounding the fluid. The free surface at $z=h$ is set with vanishing shear stress. On the solid walls at $z=0$ and $r=1$, the no-slip conditions are applied in Section 4.1, where the symptom of the inertial oscillation caused by the corner vortex in the actual spin-up flows is presented, and the fluid's slip is permitted in Section 4.2, where the numerical solutions for the behavior of isolated vortices without being bothered by the presence of the solid boundaries are presented.

The initial conditions for the equations (1) and (2) are

$$v=v_0(r),\ \zeta=\zeta_0(r,\ z)\ \text{at}\ t=0 \tag{6}$$

In Section 4.1 we specify $v_0=-r$ and $\zeta_0=0$ corresponding to the spin-up from rest. In Section 4.2 we set essentially an arbitrary profile for v_0 and set $\zeta_0=0$ all over the domain except within one or two small circles in which uniform vorticity is specified.

To enhance the grid resolution near the bottom wall, an exponential function is used with two parameters b and z_0;

$$\eta=z-z_0(b-1)\,(e^{-z/z_0}-1)$$

where η is a new variable to be used in the numerics with a unform grid size.

The governing equations (1) through (3) are discretized by the centered difference method and the time integration for the ζ-equation is performed by the forth-order Runge-Kutta method, while the stream function equation is solved by a conjugate gradient method.

2.2 One-Dimensional equations with an improved ekman pumping model

When the Rossby number ε is small enough, the Taylor-Proudman theorem applies and the quasi-geostrophic flow is governed by

$$\frac{\partial V}{\partial t}+U\frac{\partial V}{\partial r}+\frac{UV}{r}+\frac{2}{\varepsilon}U=\frac{1}{Re}\triangle_1 V \tag{7}$$

where U and V denote the depth averages of u and v, respectively, and $\triangle_1=\partial^2/\partial r^2+\partial/r\partial r-1/r^2$. The radial velocity component U is given by the integration of the continuity equation in terms of the Ekman pumping velocity w_E from the edge of the boundary layer near the bottom wall;

$$U=\frac{1}{hr}\int_0^r rw_E dr \tag{8}$$

Analysis for the bottom boundary-layer flow provides the Ekman pumping velocity w_E;

$$w_E=\frac{1}{2}\sqrt{\frac{\varepsilon}{Re}}\left[\left(\frac{\partial V}{\partial r}+\frac{V}{r}\right)-\varepsilon\left(\frac{9}{80}\frac{V}{r}\frac{\partial V}{\partial r}+\frac{7}{80}V\frac{\partial^2 V}{\partial r^2}+\frac{7}{80}\frac{\partial V}{\partial r}\frac{\partial V}{\partial r}\right)\right] \tag{9}$$

Note that the first term on the right-hand side corresponds to the classical linear pumping model. The higher-order correction on the right-hand side is in fact consistent with that derived by Hart (2000) except that his paper has typographical errors.

Although U at the side wall is in principle zero, a small non-zero of U at this wall can lead to the overall numerical instability. Thus, at every time step we subtract from w_E the averaged quantity $\bar{w}$ defined as

$$\bar{w}_E=2\int_0^1 rw_E dr \tag{10}$$

2.3 Analysis for one-dimensional inviscid flows with linear pumping law

If the linear pumping law is considered, U becomes from (8) and (9)

$$U=\frac{\sqrt{E}}{2h}V$$

where $E=\varepsilon/Re$ indicates the Ekman number based on the radius of the cylinder (not on the liquid depth). Substituting this into the inviscid version of (7) gives

$$\frac{\partial V}{\partial t}+\frac{\sqrt{E}}{2h}\left(V\frac{\partial V}{\partial r}+\frac{V^2}{r}+\frac{2}{\varepsilon}V\right)=0$$

This equation admits a separation-of-variables form as a solution. It can be shown that the solution can be written as

$$V=\frac{-r}{(1-\varepsilon)e^{\sqrt{E}t/h\varepsilon}+\varepsilon} \tag{11a}$$

for $r<r_c$, and

$$V=\frac{r-1/r}{\varepsilon(e^{\sqrt{E}t/h\varepsilon}-1)} \tag{11b}$$

for $r\geq r_c$, where r_c is determined by

$$r_c=[1-\varepsilon+\varepsilon e^{-\sqrt{E}t/h\varepsilon}]^{1/2} \tag{12}$$

The above solutions are firstly derived by Wedemeyer (1964), and later by Maas (1993) and van de Konijnenberg and van Heijst (1995).

3. Inertial Oscillations

The most important phenomenon in association with the motion of the azimuthal vortices under the background rotation is the 'inertial oscillation' or the 'inertial wave' (see e.g. Greenspan, 1968). The time scale of the inertial motion is much smaller than the one of the advection in the axial plane at low Rossby numbers. Thus in the inviscid and low-Rossby-number limit, the only terms which make balance with the Coriolis terms in equations (1) and (2) are $\partial v/\partial t$ and $\partial\zeta/\partial t$. Then (1) and (2) reduce to

$$\frac{\partial v}{\partial t}=-\frac{2}{\varepsilon}u \tag{13a}$$

$$\frac{\partial\zeta}{\partial t}=-\frac{2}{\varepsilon}\frac{\partial v}{\partial z} \tag{13b}$$

Eliminating v from these two gives

$$\frac{\partial^2\zeta}{\partial t^2}=\frac{4}{\varepsilon^2}\frac{\partial u}{\partial z} \tag{14}$$

In terms of the stream function this is written as

$$\frac{\partial^2}{\partial t^2}\triangle_2\psi+\frac{4}{\varepsilon^2}\frac{\partial^2\psi}{\partial z^2}=0 \tag{15}$$

The separable form of the solution can be expressed as

$$\psi=e^{l(st+kz)}J_1(lr) \tag{16}$$

where k is the wave number along the z-direction, l corresponds to the wave number along the r-direction, and s is the frequency given by

$$s=\frac{2k}{\varepsilon\sqrt{k^2+l^2}} \tag{17}$$

Typically the frequency s is of $O(1/\varepsilon)$. Also note that the frequency takes a maximum value

$$s_{\max}=\frac{1}{\varepsilon}$$

when the flows in the axial plane are purely radial, i.e. $l=0$, while it becomes zero, or the flows are steady, when the streamlines are vertical, i.e. $k=0$. Otherwise, the wave propagates vertically with the phase velocity s/k, or $2/(\varepsilon\sqrt{k^2+l^2})$. Thus the mode propagates faster at lower Rossby numbers.

Equation (14) also implies that vertical gradient in the radial velocity u causes an increase of the time rate of the azimuthal vorticity ζ. Therefore, even when the flow field is initially irrotational, if there is a region where the radial velocity has a vertical gradient, then a vorticity field is induced in the region as will be shown in the following section.

4. Results of the Numerical Computations

4.1 Spin-up flows within a circular cylinder

The two-dimensional numerical computations for the spin-up process of a viscous fluid in a circular cylinder are performed with grids 201×101 at $Re=10000$, $\varepsilon=h=0.5$ and with grids 301×151 at $Re=30000$, $\varepsilon=h=0.5$. For the strain of the z-coordinate, $b=3$ and $z_0=0.1$ are chosen. In most cases $\Delta t=0.01$ gives the converged solutions. These computational experiments are purposed firstly to verify the numerical

field (as shown in Figs. 7 and 9, and Table 2). This is also the reason why slip factors with conventional models are closer to area-averaged value than to mass-averaged value based on CFD results.

Consequently, with actual significance and final interest, predicted circumferential components of absolute velocity with slip factor models are compared with mass-weighted and area-weighted averaged velocities based on CFD results. As shown in Fig. 10, the mass-averaged absolute circumferential velocity evaluated from CFD results is greater than area-averaged value by over 20 percent, and the discrepancy increases with the flow coefficient, which implies that the backflow within impeller becomes stronger as the flow coefficient increases. All of the predicted absolute circumferential velocities with various slip factor models are still closer to area-averaged values in entire flow rate range. Although the slip factor with Eck model is closest to mass-averaged value in Fig. 7, in this case for absolute circumferential velocity shown in Fig. 10, Eck model gives rather poor results.

It is found, in Figs. 7(b) and 10(a), that the slip factor model developed in this work predicts slip factor and absolute circumferential velocity closest to area-averaged values among the slip factor models tested in this work. Especially, at the flow rate where peak total pressure coefficient of impeller takes place (φ=0.265), predicted absolute circumferential velocity with present model agrees with area-averaged value very well. The agreement between predicted absolute circumferential velocity with present model and the area-averaged value based on CFD results is within 2.3 percent for entire range of flow rate considered in this work. The fact that the predictions with the present model agree well with the area-averaged values rather than the mass-averaged values, implies that the present slip factor model can provide accurate prediction for absolute velocity in case with rather uniform distribution of flow within blade passage.

The correction method developed in this work is coupled with slip factor models to predict absolute circumferential velocities in Fig. 11. In comparison with Fig. 10, it is found that the predictions with the slip factor models are improved by the correction method, and thus become closer to the mass-averaged value rather than the area-averaged value except the case of Eck model. In most of the flow rate range, together with the correction method, Stodola and Wiesner models overestimate the mass-averaged absolute circumferential velocities slightly. The agreement between predictions and the CFD results are within 10.7 percent for Stodola model, and 5.6 percent for Wiesner model in entire range of flow rate

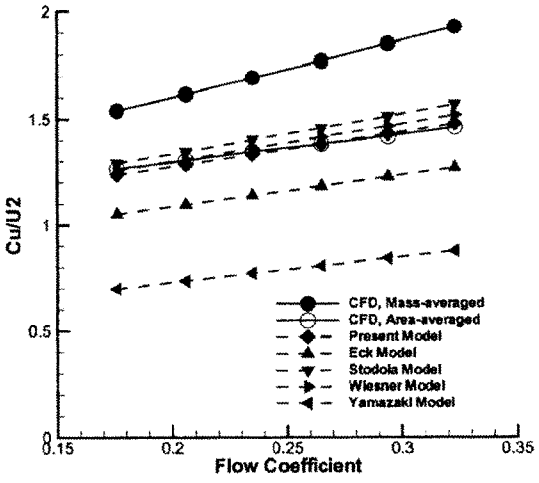

Fig. 10 Comparison of predicted circumferential-averaged velocity at exit of impeller

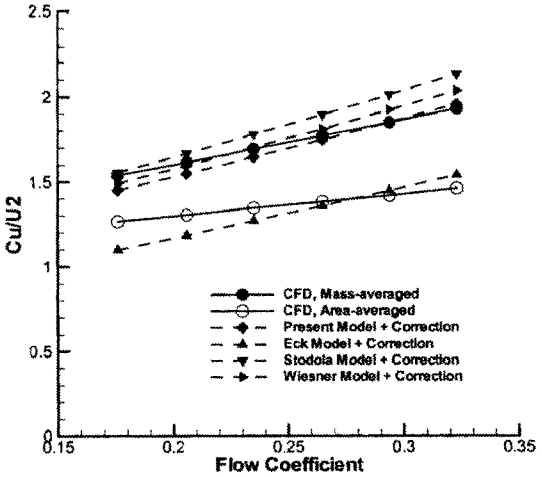

Fig. 11 Predicted $\bar{C}_{u2}$ at exit of impeller

however evolve very fast and the evolution is not characterized by advection but by inertial waves or oscillations.

Figure 3 shows the temporal behavior of $v(0.7, h, t)$ and $v(0.7, h/2, t)$ up to $t=20$ given by the two-dimensional numerics for $\varepsilon=0.2$ and 0.5. It clearly exhibits the oscillatory motions the period being much shorter than the spin-up time scale $O(\sqrt{E}/h\varepsilon)$. It also demonstrates the higher frequency at lower Rossby numbers in line with the analysis presented in the previous section. On the other hand, the fundamental assumption behind the Ekman pumping models proposed hitherto is that the radial component of velocity remains z-independent, except of course *in the Ekman boundary-layer on the bottom* wall. In this sense the considerable variation of u shown in the axial plane (Figure 2) may cast doubt on the validity of the model. Some authors (e.g. Zavala, Sanson and van Heijst, 2000) suggest to use depth-averaged quantities instead of requiring the z-independency; however the resultant equations for the fluid motions in the axial plane are the same as far as the effect of the oscillatory motions is not considered.

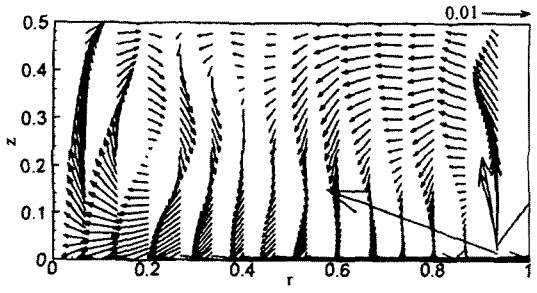

(a) $t=15$

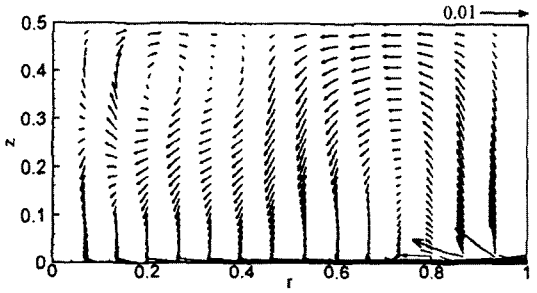

(b) $t=45$

Fig. 2 Velocity vectors in the axial plane computed by two-dimensional numerics for the same parameter set as figure 1

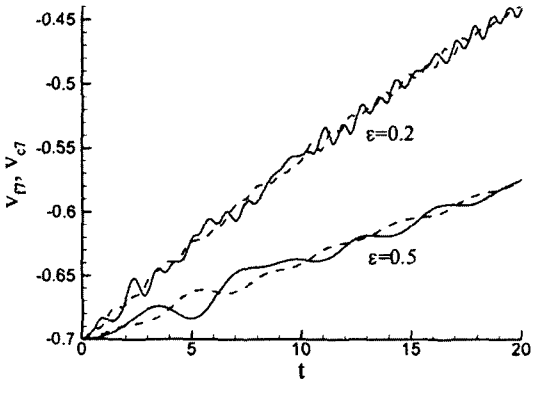

Fig. 3 History of v_{f7} (the azimuthal velocity component evaluated at $r=0.7$ and at $z=h$, i.e. at the free surface; solid lines) and v_{f7} (the one at $r=0.7$ and $z=h/2$; dashed lines), given by two-dimensional numerics for the same parameter set as figure 1

Figure 4 shows the time average of the velocity vectors presented in Figure 2. We can see that in the region $r>0.4$ the radial component u is almost uniform along the vertical coordinate. This means that the z-independent nature of u is guaranteed only in a time-average sense or in the spin-up time scale but not in the time scale of the inertial oscillations. Then the next question is; what will be the effect of the inertial oscillation on the momentum transfer between the Ekman layer and the bulk fluid? This issue may play one of the key roles in improvement of the Ekman-pumping model.

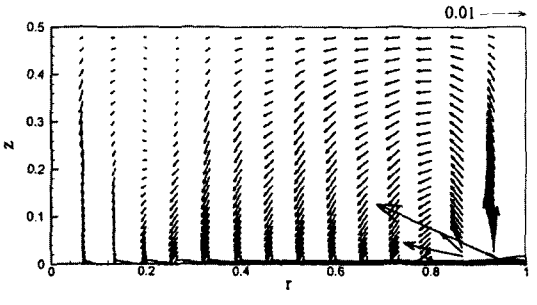

Fig. 4 Velocity vectors in the axial plane averaged for $30-2\pi \leq t \leq 30$ given by two-dimensional numerics for the same parameter set as figure 1

Figure 5 shows a sequence of initial developments of the streamlines and the azimuthal vorticity contours in the axial plane. This sequence reveals the generation mechanism of the inertial waves. At first ($t=2$), a corner vortex is generated by the roll-up of the vortex sheet of positive vorticity on the bottom wall. Due to the image vortex behind the side wall as well as the strong blowing from the Ekman boundary-layer, this vortex moves up ($t=3$). As a result, the fluid situated in the left-hand side of this vortex moves down toward the right-hand side and then turn to the left to be finally sucked into the Ekman boundary-layer on the bottom wall ($t=3$). On the other hand the region very close to the vortex core at the left-down side (i.e. near $r=0.9$ and $z=0.1$ at $t=2$) is characterized by a negative value in $\partial u/\partial z$. As shown in the previous section (via the equation (14)) this gradient induces a negative vorticity in the same place ($t=3, 4$). The vortex is propagated upward and toward the wall while becoming slender. Simultaneously in the region between the mentioned vortex and the bottom wall a positive vorticity is generated ($t=5$). After this, the mentioned positive vortex pattern travels toward the wall while inducing another negative vortex behind it, and so on. Although the vortices' propagation is toward the side wall, the movement of the fluid element is toward the central region in a time-average sense as shown in Figure 4. Vortical flows become more pronounced in the core at later time (see Figure 2); we can see from Figure 4 that a slightly wavy pattern still exists in the core even if the velocity components are time-averaged.

Hitherto we have seen the axisymmetric flow evolutions in the actual spin-up flows. In summary, the complex flow pattern shown in the axial plane is caused by the mechanism of inertial oscillation the perturbation being the corner vortex generated at the beginning of the spin-up process. The corner vortex is of course generated by both the Ekman circulation and the bottom friction. In the next section, to focuss our attention on the motion of the azimuthal vortex we will consider a single vortex or a pair of vortices, in a form of vortex patch, without the Ekman circulation or frictions of the bottom and side walls.

4.2 Motion of azimuthal vortices under a background rotation

Figure 6 shows the time evolution of streamlines and vorticity contours obtained by the numerical computation of (1) through (3) now with homogeneous boundary conditions

$$v=\psi=\zeta=0 \text{ at } r=0,\ 1 \tag{18a}$$

$$\frac{\partial v}{\partial z}=\psi=\zeta=0 \text{ at } z=0,\ h \tag{18b}$$

The flow is induced only by a circular vortex-patch of radius 0.05 having a uniform vorticity with magnitude $\zeta_0=1$ situated initially at the position, $r=0.9$ and $z=0.2$, in the similitude of the corner vortex shown in Figure 5; otherwise, the entire domain is initially quiescent. All the other parameter values used in the computation is the same as Figure 1. Since the boundary conditions on the lower and side walls are set as (18a) and (18b), slip of the fluid element is permitted on the walls. Thus, we have neither Ekman pumping effect from the lower wall nor friction effect on the side wall so that we can study the vortical motions in a completely solitary status.

The only no-slip condition at the side wall, i.e. the condition at the wall $r=1$, shown by the equation (18a) in fact exerts no fundamental effect on the vortices' dynamics because the boundary layer adjacent to the side wall caused by the no-slip condition for v remains very thin, being attached to the wall during the course of the vortical development.

At $t=1$ most of the domain is characterized by a weak stream except near the side wall where the vortex patch resides; since the vortex patch is initially positive, the vortical flow in this region is counterclockwise. At $t=2$ however the flow direction is reversed because the central region of the vortex patch is switched from positive to negative vorticity. It can be shown that for a small circular patch the vorticity keeps its uniform distribution but the magnitude is changed repeatedly with the angular frequency $2/\varepsilon$. On the other hand each of the vortices with negative vorticity

generated on the right-and left-hand sides respectively of the initial patch (shown at $t=1$) tends to take a 'X' shape ($t=3$) and is pushed toward the side wall. Near $r=0.8$ and $z=0.2$

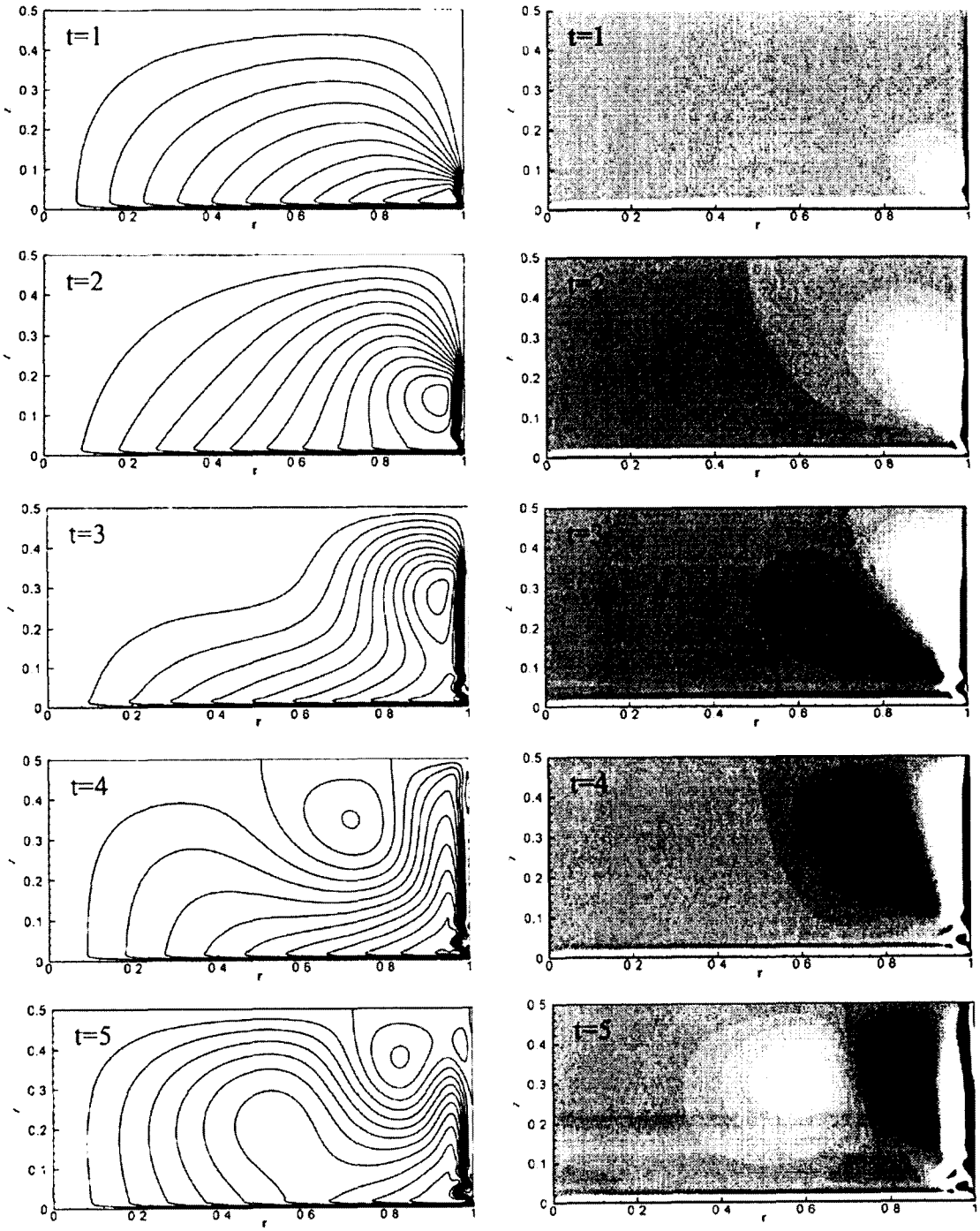

Fig. 5 Streamlines (left) and vorticity countours (right) obtained by two-dimensional numerics for the same parameter set as figure 1. Increment of stream functions is 0.0002, and the vorticity is colored white for the value greater than 0.2 and black for lower than -0.2

another vortex with positive vorticity is generated ($t=3$) and rapidly grows to be split into two

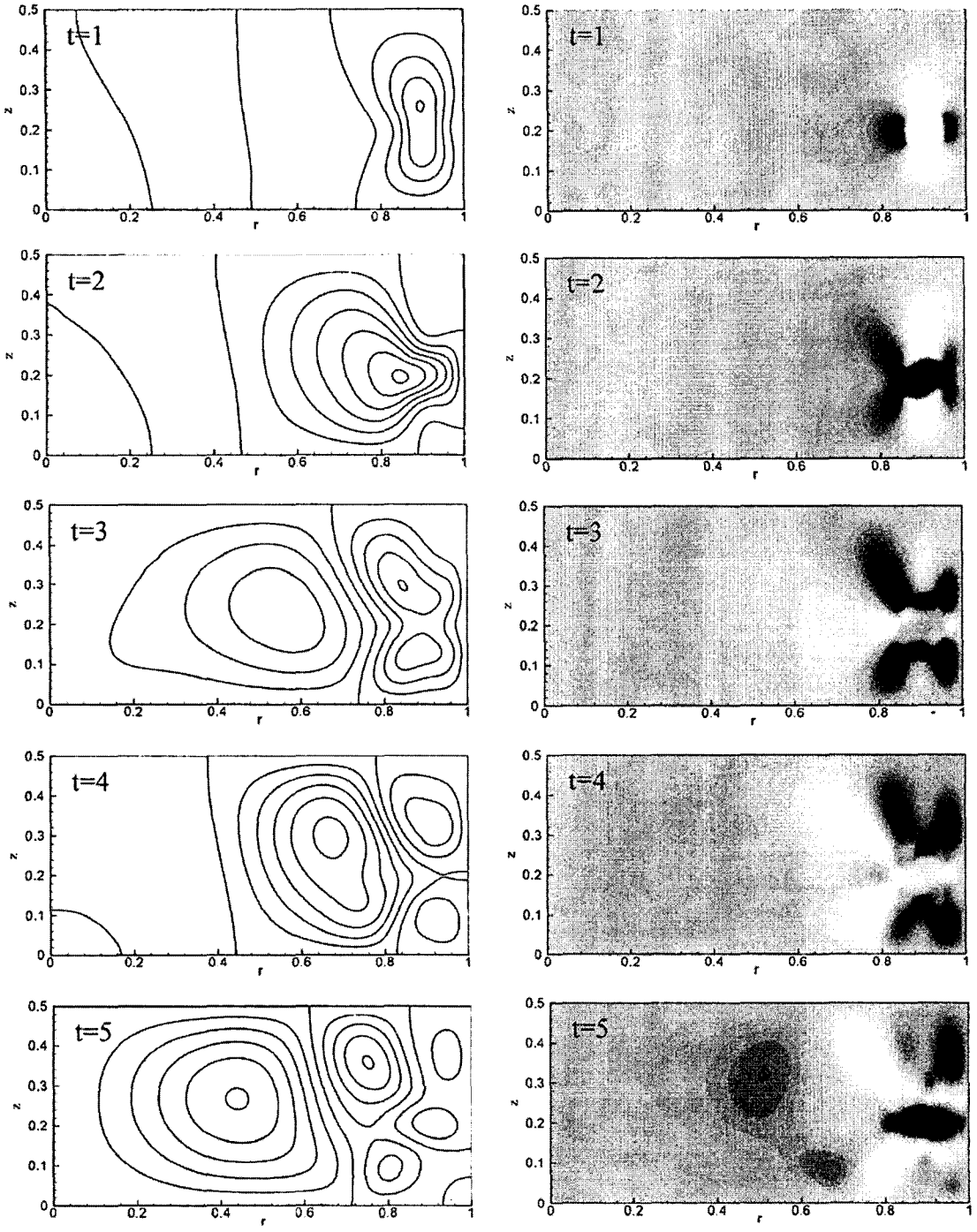

Fig. 6 Streamlines (left) and vorticity countours (right) obtained by two-dimensional numerics for the case with single vortex patch of initial $\zeta_0=1$ under the slip boundary conditions on the solid walls; $Re=30000$, $h=\varepsilon=0.5$. Increment of stream functions is 0.0002, and the vorticity is colored white for the value greater than 0.2 and black for the one lower than -0.2

(t=4). At t=5 near r=0.5 and z=0.3 another vortex with negative vorticity is also generated.

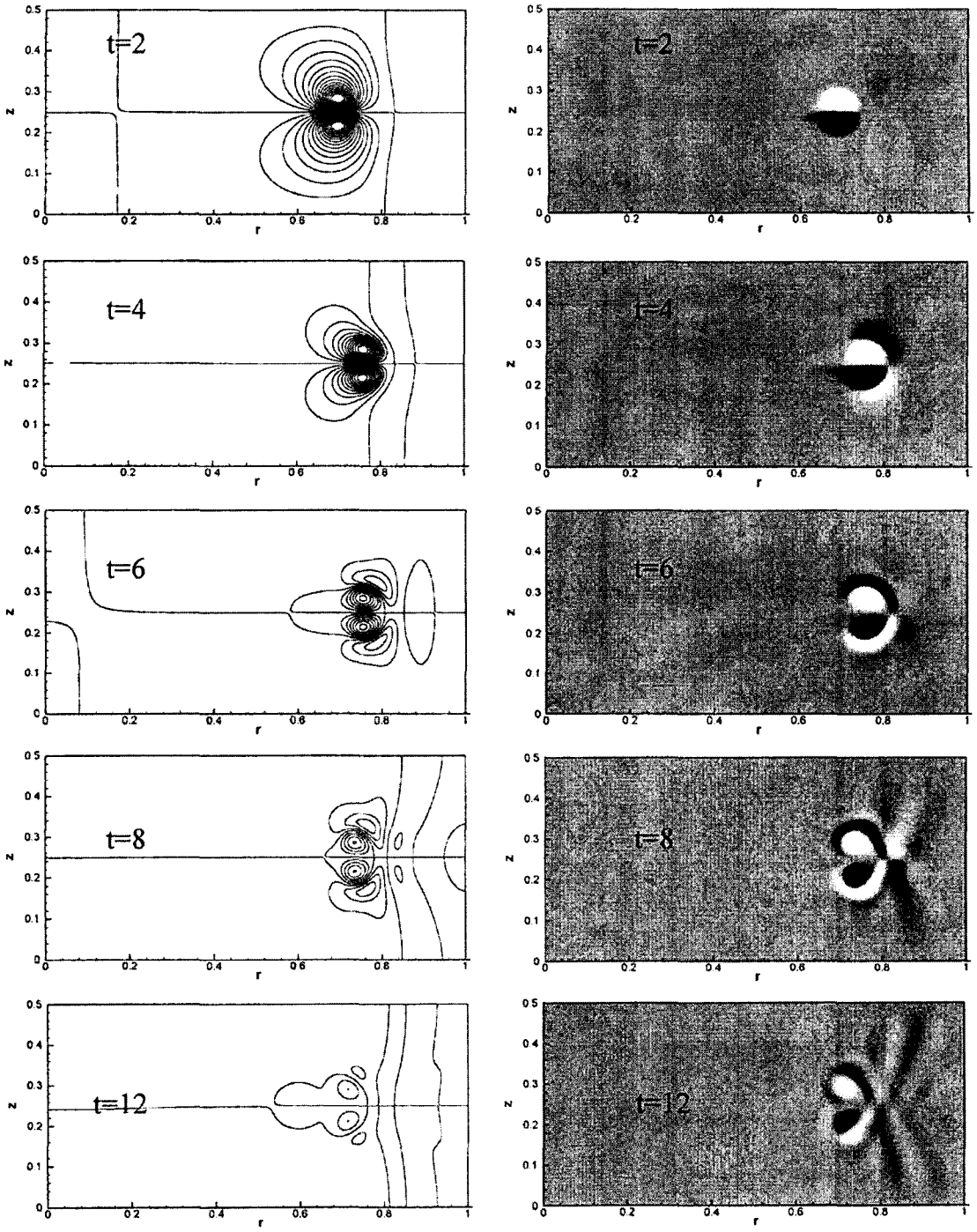

Fig. 7 Streamlines (left) and vorticity countours (right) obtained by two-dimensional numerics at Re=30000, ε=1 and h=ε=0.5 with the initial azimuthal velocity distribution and the intial vorticity as specified in the text for the slip boundary conditions on the solid walls. Increment of stream functions is 0.0002, and the vorticity is colored white for the value greater than 1.0 and black for lower than −1.0

Although the vorticity generation point moves with time toward the central axis, all the vortices propagate toward the side wall. In fact, Figure 6 implies that the continuous generation of the azimuthal vortices and subsequent oscillations in the flow field shown in Figure 5 is basically due to the corner vortex (shown at $t=2$ and 3 in Figure 5), the result of roll-up of the positive-vorticity sheet on the Ekman boundary-layer.

Figure 7 shows the numerical results for the case when a pair of vortices, with opposite signs of vorticity with magnitudes $\zeta_0=\pm 10$, was situated initially at $r=0.6$, $z=h/2\pm 0.03$. The initial azimuthal velocity v_0 was set as

$$v_0=\begin{cases} -r & \text{for } r\leq 0.75 \\ B(r-r^{-13/11}) & \text{for } r>0.75 \end{cases}$$

where B is chosen in such a way that the profile is continuous at $r=0.75$. The profile for the outer region is similar to (11b), but here it was obtained through the linear analysis to the inviscid version of (7) with the first-order correction for the Ekman pumping law included. Since the Rossby number in this case is 1, this profile in fact mimics the azimuthal velocity distribution of the spin-up from rest at the time when the front reaches $r=0.75$, which was arbitrarily chosen. The core region bounded by the front therefore has a zero azimuthal velocity in the inertial frame of reference, and thus the vortices (these vortices will be referred to as 'primary' hereafter) simply move radially outward until they reach the front $r=0.75$. After the contact, however, the evolution is quite different from the ordinarily observed pattern. As soon as the vortices contact the border, they are surrounded by a pair of crescent-shape vortices on the outer-region side, which are of course generated by the primary vortices; see the frames for $t=2$ in Fig. 7. As a result, the primary vortices become almost stationary afterward. During and after this event, the outer region is disturbed by the presence of the primary vortices and shows the inertial waves as seen in Fig. 7, especially after $t=8$. This means that the outer region is characteristic of rotating flows, whereas the core region is free from the rotational effect. We can also observe that the primary vortices weaken very rapidly after they reside at the border, as can be distinctively captured from the streamline patterns.

Penetration of vortices from the core to the outer region may be realized by, for instance, ejecting a vortex ring into a rotating fluid during a spin-up process from the bottom of the container at the time when the front reaches $r=0.75$. In this case the vortex ring at first may travel all the way up to the free surface of the fluid and then turn toward the outer region. Preparation for the experimental study on such occasion is currently performed in the author's laboratory.

5. Conclusions

It was shown that the two-dimensional computation for the spin-up flow within a circular cylinder is in close agreement, in the core region between the rotational axis and the front, with the one-dimensional computation with an Ekman pumping model which includes the first-order correction. In the outer region between the front and the side wall, however, the discrepancy is considerable, and the profile given by the two-dimensional numerics is smoother than that given by one-dimensional computation. At $\varepsilon=0.5$, the axial plane is dominated by the typical inertial-wave motion superimposed by the well known Ekman circulation in the spin-up process. The wave motions turn out to be stronger than expected. However they do not deteriorate, in a time scale larger than the period of inertial-oscillations, the underlying assumption for the classical Ekman pumping law; that is, the radial velocity component is uniform over and the vertical component is proportional to the depth from the free surface, in the inviscid region.

When a small vortex patch is introduced at $\varepsilon=0.5$ without any other perturbation, the vorticity changes its sign repeatedly and the whole flow field in the axial plane is dominated by a complex inertial-wave pattern. Finally, when a pair of small vortex patches is introduced with initial distribution of azimuthal velocity component in two steps, which mimics the situation of a spin-up from rest, the motion of vortices is completely

different for the core and outer regions. At the initial stage when the pair is at the core region, it simply moves straight outward. As soon as the outer region is touched by the pair vortices at the border, it blocks the vortices' penetration by surrounding them with the crescent-shape vortices, making the pair motionless. The outer region is then dominated by the typical inertial waves, and the pair vortices weaken very fast.

In the future, numerical computations for the pair vortices' motion at various initial distribution of the azimuthal velocity component are required to investigate its effect on the motion of the pair vortices as well as on the inertial-wave structure. The final goal in the series of studies on the inertial oscillations and vortical motions is to develop an improved Ekman pumping model which has a broad range of applications in the fluid mechanics area.

Acknowledgment

This work was supported by the Dong-A University Research Fund in 2002. This work has also been supported by grant No. R12-2002-058-01004-02003 from the CANSMC of KOSEF.

References

Cederlöf, U., 1988, "Free-Surface Effects on Spin-up," *J. Fluid Mech.*, Vol. 187, pp. 395~407.

Dolzhanskii, F. V., Krymov, V. A. and Manin, D. Y., 1992, "Self-Similar Spin-up and Spin-down in a Circular Cylinder of Small Ratio of Height to Diameter," *J. Fluid Mech.*, Vol. 234, pp. 473~486.

Greenspan, H. P., 1968, *The Theory of Rotating Fluids*, Cambridge University Press.

Greenspan, H. P. and Howard, L. N., 1963, "On a Time Dependent Motion of a Rotating Fluid," *J. Fluid Mech.*, Vol. 17, pp. 385~404.

Hart, J. E., 1995, "Nonlinear Ekman Suction and Ageostrophic Effects in Rapidly Rotating Flows," *Geophys. Astrophys. Fluid Dynamics*, Vol. 79, pp. 201~222.

Hart, J. E., 2000, "A Note on Nonlinear Correction to the Ekman Layer Pumping Velocity," *Phys. Fluids*, Vol. 12, No. 1, pp. 131~135.

Hyun, J. M., Fowlis, W. W. and Warn-Varnas, A., 1982, "Numerical Solutions for the Spin-up of a Strafied Fluid," *J. Fluid Mech.*, Vol. 117, pp. 71~90.

Maas, L. R. M., 1993, "Nonlinear and Free-Surface Effects on the Spin-down of Barotropic Axisymmetric Vortices," *J. Fluid Mech.*, Vol. 246, pp. 117~141.

Suh, Y. K. and Choi, Y. H., 2002, "Study on the Spin-up of Fluid in a Rectangular Container Using Ekman Pumping Models," *J. Fluid Mech.*, Vol. 458, pp. 103~132.

van de Konijnenberg, J. A. and van Heijst, G. J. F., 1995, "Nonlinear Spin-up in a Circular Cylinder," *Phys. Fluids*, Vol. 7, No. 12, pp. 2989~2999.

Wedemeyer, E. H., 1964, "The Unsteady Flow within a Spinning Cylinder," *J. Fluid Mech.*, Vol. 20, pp. 383~399.

Zavala Sanson, L. and van Heijst, G. J. F., 2000, "Nonlinear Ekman Effects in Rotating Barotropic Flows," *J. Fluid Mech.*, Vol. 412, pp. 75~91.